Human Reproduction, Vol.33, No.1 pp. 128–139, 2018
Advanced Access publication on November 28, 2017 doi:10.1093/humrep/dex338

human reproduction

ORIGINAL ARTICLE *Reproductive endocrinology*

Chronic hyperandrogenemia in the presence and absence of a western-style diet impairs ovarian and uterine structure/function in young adult rhesus monkeys

Cecily V. Bishop[1], Emily C. Mishler[1], Diana L. Takahashi[2], Taylor E. Reiter[1], Kise R. Bond[1], Cadence A. True[2], Ov D. Slayden[1,2,3], and Richard L. Stouffer[1,2,3,*]

[1]Division of Reproductive & Developmental Sciences, Oregon National Primate Research Center, Oregon Health & Science University, Beaverton, OR 97006, USA [2]Cardiometabolic Health Division, Oregon National Primate Research Center, Oregon Health & Science University, Beaverton, OR 97006, USA [3]Obstetrics & Gynecology, Oregon Health & Science University, Portland, OR 97239, USA

*Correspondence address. E-mail: stouffri@ohsu.edu

Submitted on August 23, 2017; resubmitted on October 13, 2017; accepted on October 19, 2017

STUDY QUESTION: Does chronic hyperandrogenemia beginning at menarche, in the absence and presence of a western-style diet (WSD), alter ovarian and uterine structure-function in young adult rhesus monkeys?

SUMMARY ANSWER: Phenotypic alterations in ovarian and uterine structure/function were induced by exogenous testosterone (T), and compounded in the presence of a WSD (T+WSD).

WHAT IS KNOWN ALREADY: Hyperandrogenemia is a well-established component of PCOS and is observed in adolescent girls, indicating a potential pubertal onset of disease symptoms. Obesity is often associated with hyperandrogenemia and it is hypothesized that metabolic dysfunction exacerbates PCOS symptoms.

STUDY DESIGN, SIZE, DURATION: Macaque females ($n = 40$) near the onset of menarche (~2.5 years of age) were assigned to a 2 by 2 factorial cohort design. Effects on reproductive characteristics were evaluated after 3 years of treatment.

PARTICIPANTS/MATERIALS, SETTING, METHODS: Rhesus macaques (*Macaca mulatta*) were fed either a normal balanced diet ($n = 20$) or a WSD ($n = 20$). Additionally, implants containing cholesterol ($n = 20$) or T ($n = 20$) were implanted subcutaneously to elevate serum T approximately 5-fold. This resulted in treatment groups of controls (C), T, WSD and T+WSD ($n = 10$/group). Vaginal swabbing was performed daily to detect menses. After 3 years of treatment, daily serum samples from one menstrual cycle were assayed for hormone levels. Ovarian structure was evaluated in the early follicular phase by 3D/4D ultrasound. Uterine endometrial size and ovarian/luteal vascular function was also evaluated in subgroups ($n = 6$/group) in the late follicular and mid-luteal phases by 3D/4D ultrasound and contrast-enhanced ultrasound, respectively. Expression of steroid hormone receptors and markers of decidualization and endometrial receptivity were assessed in endometrial biopsies at mid-luteal phase.

MAIN RESULTS AND THE ROLE OF CHANCE: Approximately 90% of menstrual cycles appeared ovulatory with no differences in frequency or duration between groups. Serum estradiol (E2) levels during the early follicular phase were greatest in the T alone group, but reduced in T+WSD ($P < 0.02$). Serum LH was elevated in the T group ($P < 0.04$); however, there were no differences among groups in FSH levels ($P > 0.13$). Ovarian size at menses tended to be greater in the WSD groups ($P < 0.07$) and antral follicles ≥1 mm were more numerous in the T+WSD group ($P < 0.05$). Also, females in T and T+WSD groups displayed polycystic ovarian morphology (PCOM) at greater frequency than C or WSD groups ($P < 0.01$). Progesterone (P4) levels during the luteal phase were reduced in the T+WSD group compared to C and T groups ($P < 0.05$). Blood volume (BV) and vascular flow (VF) within the corpus luteum was reduced in all treatment groups

compared to C ($P < 0.01$, $P = 0.03$), with the WSD alone group displaying the slowest BV and VF ($P < 0.05$). C and WSD groups displayed endometrial glands at mid-luteal phase with low estrogen receptor 1 (ESR1) and progesterone receptor (PGR) mRNA and immunohistochemical staining in the functionalis zone, but appreciable PGR in the stroma. In contrast, T and T+WSD treatment resulted in glands with less secretory morphology, high ESR1 expression in the glandular epithelium and low PGR in the stroma. Endometrial levels of TIMP3 and MMP26 mRNA and immunostaining were also decreased in the T and T+WSD groups, whereas AR expression was unchanged.

LARGE SCALE DATA: None.

LIMITATIONS, REASONS FOR CAUTION: Females are young adults, so effects could change as they reach prime reproductive age. The T level generated for hyperandrogenemia may be somewhat greater than the 3–4-fold increase observed in adolescent girls, but markedly less than those observed in male monkeys or adolescent boys.

WIDER IMPLICATIONS OF THE FINDINGS: Alterations to ovarian and uterine structure-function observed in T and, in particular, T+WSD-treated female macaques are consistent with some of the features observed in women diagnosed with polycystic ovary syndrome (PCOS), and suggest impaired fertility.

STUDY FUNDING/COMPETING INTEREST(S): Research reported in this publication was supported by the Eunice Kennedy Shriver National Institute of Child Health & Human Development (NICHD) of the National Institutes of Health (NIH) under Award Number P50HD071836 (to RLS). The content is solely the responsibility of the authors and does not necessarily represent the official views of the NIH. Additional funding was provided by Office of the Director, NIH under Award Number P51OD011092 (Support for National Primate Research Center). Authors declare no competing interests.

Key words: PCOS / hyperandrogenemia / rhesus macaque / western-style diet / obesity

Introduction

As summarized in recent reviews by Rosenfield and Ehrmann (2016) and Dumesic *et al.* (2015), polycystic ovary syndrome (PCOS) is the most prevalent endocrine disorder in reproductive-age women which, due to its associated oligo- or an-ovulation, often results in infertility. Although 80-plus years of research has increased our understanding of PCOS, considerable controversy and knowledge gaps remain regarding the etiology, symptoms, and treatment of this complex and heterogeneous disease. However, a typical feature, based on the Rotterdam, National Institutes of Health and Androgen Excess-PCOS criteria, is hyperandrogenemia resulting from elevated testosterone (T) in the circulation. Indeed, regardless of its genetic, epigenetic and/or environmental causes, there is evidence that excess ovarian androgen production is a common denominator in the vast majority of PCOS patients (Rosenfield and Ehrmann, 2016). Given that circulating androgen levels do not rise until after menarche and reach adult levels after achieving regular ovulatory cyclicity (Rosenfield, 2013), one can hypothesize that other features of PCOS are caused by the chronic hyperandrogenemia beginning at puberty and, as such may be treatable at that time.

In addition to ovarian dysfunction, a majority of PCOS patients are obese or overweight and display insulin resistance (Dumesic *et al.*, 2015; Rosenfield and Ehrmann, 2016). Some investigators propose that metabolic abnormalities related to obesity are just as, if not more, critical than hyperandrogenemia for reproductive dysfunction, including acyclicity and oocyte quality (Palomba *et al.*, 2017). Also, Dumesic and others (Dumesic *et al.*, 2015; Rosenfield and Ehrmann, 2016) hypothesize that obesity and adipose tissue dysfunction exacerbates the symptoms of PCOS. Notably, obesity is associated with hyperandrogenemia in peripubertal girls, suggesting an early link between metabolic and reproductive defects (Hoeger *et al.*, 2008). Tissue dysfunction in PCOS is not exclusively ovarian or adipose: PCOS may alter function of the endometrium, effecting receptivity and embryo implantation (Schulte *et al.*, 2015). Therefore, a systems approach to investigate how adipose, ovarian and uterine tissue are impacted by PCOS is warranted.

An important question then is discerning how putative causative factors, such as elevated T or metabolic perturbations, interact to produce PCOS symptoms. In our recent pilot study (McGee *et al.*, 2014; Bishop *et al.*, 2016), combined administration of T with an obesogenic western-style diet (WSD) decreased insulin sensitivity and altered features of ovarian function in female rhesus monkeys. Although the protocol provided intriguing evidence for some PCOS-like effects of chronic T+WSD treatment, it was limited in experimental design and unable to distinguish effects of T or WSD alone, or if the effects of T and WSD were additive or synergistic. Therefore, this more rigorous study was designed to examine the effects of T alone, WSD alone, or T+WSD together compared to controls in juvenile-to-young adult female macaques. The WSD was formulated with 36% of calories from fat, compared to 15% in the standard chow diet (True *et al.*, 2017). Treatment began as the monkeys approached menarche, and data accumulated through 3 years of treatment have been analyzed. The metabolic impairments (True *et al.*, 2017) and changes in adipose tissue (Varlamov *et al.*, 2017) in this model were reported recently. The effects on the ovarian-uterine axis are reported herein, while an ongoing study (Bishop *et al.*, 2017c) is underway evaluating the effects on the peri-ovulatory follicle.

Materials and Methods

Animals

All procedures involving animals were reviewed and performed in accordance with the Oregon National Primate Research Center/Oregon Health & Science University Institutional Animal Care and Use Committee. Rhesus macaque (*Macaca mulatta*) females ($n = 40$) were pair-housed indoors and assigned to treatment groups near menarche (Table I).

Table I Menstrual cycles by year of treatment in control (C), testosterone (T), western-style diet (WSD) and T+WSD groups.

Study interval/ year	Treatment group*	# Cycles	Cycle length (days)	% Ovulatory cycles[a]	Age at assignment (years)	Age at menarche (years)
1	C	5.2 ± 0.5[A]	44.5 ± 3.1[A]		2.3 ± 0.1	2.4 ± 0.1
	T	4.4 ± 0.7[A]	48.9 ± 4.1[A]		2.2 ± 0.1	2.5 ± 0.1
	WSD	5.3 ± 0.5[A]	49.7 ± 5.4[A]		2.5 ± 0.1	2.7 ± 0.1
	T+WSD	4.3 ± 0.8[A]	46.0 ± 4.3[A]		2.2 ± 0.1	2.7 ± 0.1
2	C	9.3 ± 0.5[B]	28.8 ± 1.3[B]			
	T	9.2 ± 0.4[B]	28.2 ± 0.6[B]			
	WSD	9.0 ± 0.6[B]	30.8 ± 2.1[B]			
	T+WSD	8.8 ± 0.8[B]	32.7 ± 4.6[B]			
3	C	9.0 ± 0.3[B]	28.2 ± 1.2[B]	94 ± 3.0		
	T	9.2 ± 0.4[B]	27.8 ± 0.9[B]	90 ± 6.5		
	WSD	8.8 ± 0.6[B]	27.3 ± 0.7[B]	89 ± 6.3		
	T+WSD	8.9 ± 0.6[B]	28.0 ± 0.9[B]	85 ± 6.8		

*n = 10 female macaques per treatment group; values mean ± SEM.
[a]Number of ovulatory cycles only recorded during Study Year 3.
Uppercase letters indicate differences (A vs B; $P < 0.001$) within each group by year of treatment.

Menarche was determined by first onset of frank vaginal bleeding. Animals were fed either a standard control macaque diet (C) or western-style diet (WSD). The C diet (Monkey Diet no. 5000; Purina Mills, Gray Summit, MO, USA) provided approximately 15% of calories from fat; the WSD (TAD Primate Diet no. 5LOP, Test Diet; Purina Mills) provided 36% of calories from fat (Brozinick *et al.*, 2013) (Supplementary Fig. S1). Weight gain and metabolic alterations resulting from exposure to WSD are reported in our previous article (True *et al.*, 2017). Each group received a subcutaneous implant, half containing cholesterol and the other half T (Supplemental Fig. S1). In T-treated animals, serum T was maintained near 1.5 ng/ml, similar to that in our pilot study (McGee *et al.*, 2012). Mean T values in all treatment groups were reported in a companion manuscript (True *et al.*, 2017). Serum T is approximately five times higher than control females, but significantly lower than levels observed in male rhesus macaques. This resulted in the following treatment groups: C alone, T alone, WSD alone and combined T+WSD (n = 10/group; Supplemental Fig. S1). Females were monitored daily by vaginal swabbing to detect endometrial shedding denoting menstruation. After 1.5 years of treatment, weekly blood samples were obtained to assess serum levels of estradiol (E2) and progesterone (P4). Serum levels of P4 ≥ 1 ng/ml in at least one weekly sample between incidences of menses was considered indicative of an ovulatory menstrual cycle (Bishop *et al.*, 2009; Young *et al.*, 2003). Pituitary LH response to kisspeptin and GnRH challenge was assessed after 2.5 years of treatment (see Supplementary Data for methods).

Menstrual cycle analyses

Beginning in treatment Year 3 (at age 5.2 ± 0.04 years old), effects of androgen and or diet on ovarian and uterine structure-function were analyzed during one menstrual cycle. Peripheral blood samples were collected daily from unanesthetized monkeys beginning at menstruation for 30 days. Serum was stored at −20°C until assayed for steroid and gonadotropin hormones by the ONPRC Endocrine Technology Core Laboratory.

Hormone levels

Serum E2 and P4 levels were measured in daily samples in the interval between onset of frank menstruation (Day 1) and onset of next menses. Anti-Müllerian hormone (AMH), FSH and LH levels were measured during the early follicular phase (Days 1–3) and late luteal phase (3 days preceding the next menstruation). Serum LH levels were measured daily 2 days before, the day of, and the day after the E2 peak. Lengths of follicular and luteal phase were denoted from the day of the mid-cycle LH surge (day of LH surge = Day 0 of luteal phase). Mid-luteal production of LH and E2 was measured on Days 6–8 of the luteal phase. All hormones were assayed using validated methods for macaque serum (McGee *et al.*, 2012, 2014).

Ultrasound analyses

Ovarian structure in the early follicular phase (Days 1–3; ovarian size, number of antral follicles, antral follicle location within the ovary) was analyzed in all females (n = 10/group) by 3D/4D Doppler ultrasound (GE Voluson 730 Expert, GE Healthcare, Milwaukee, WI, USA) under ketamine sedation (10 mg/kg) using previously validated methods (Bishop *et al.*, 2009; McGee *et al.*, 2014). Polycystic ovarian morphology (PCOM) was determined for each ovary using defined characteristics (Bishop *et al.*, 2016). Near the mid-cycle E2 surge and again at mid-luteal phase (6–8 days post-LH surge), a subset of monkeys (n = 6/group) were sedated with ketamine and placed under inhaled isoflurane anesthesia (1.5% isoflurane mixed with 100% oxygen at a flow rate of 1.5 l/min; Portable Anesthesia Machine, Patterson Veterinary Supply, Inc. Greeley, CO, USA). Ovarian/luteal and uterine (basalis zone and endometrial) vascular parameters including total blood volume (BV) and vascular flow (VF) were analyzed by Contrast-Enhanced Ultrasound (CEUS) employing Definity (Lantheus Medical Imaging, N. Billerica, MA, USA) microbubble intravenous infusion (Siemens Acuson Sequoia, Siemens Corporation, Washington, D.C., USA) by validated methods (Bishop *et al.*, 2014, 2017a). Endometrial and uterine volume were also measured by 3D/4D ultrasound, using the volume analysis function of 4D View Software (GE Healthcare).

Endometrial biopsies

In the mid-luteal phase (Days 6–8 post-LH surge), a subset of females (n = 7–8/group) were sedated with ketamine and placed under inhaled isoflurane anesthesia. TruCut needle biopsies of endometrium were collected by

laparoscopy. One biopsy from each animal was frozen in liquid nitrogen for RNA isolation. The remaining biopsies were embedded in Tissue Tek OCT (Sakura Finetek, Torrance, CA, USA) and frozen in liquid propane similar to previous studies (Slayden *et al.*, 1995). RNA and protein in samples were analyzed by real-time PCR and immunohistochemistry (IHC) as described below.

Immunohistochemistry

Protein expression in macaque endometrial biopsies was visualized by IHC as described previously (Brenner *et al.*, 2003; Brenner and Slayden, 2004; Slayden *et al.*, 2004). Frozen sections (6 μm) were placed on SuperFrost Plus slides (Fisher Scientific, Cat# 12-550-15, Thermo Fisher Scientific, Waltham, MA, USA). Antibodies used were against estrogen receptor 1 (ESR1,ER-ID5; Cat#: MS-354-P, Thermo Fisher Scientific), progesterone receptor (PGR, Cat#: Ms-298-P, 1 μg, Lab Vision/NeoMarkers, Fremont, CA, USA), androgen receptor (AR-F39 (Cat#: MU256, 1/50, BioGenex, Fremont, CA, USA), Ki67 (Cat#: MU370-UC, 1/200, BioGenex), MMP26 (Cat# ab57636; Abcam, Cambridge, MA, USA) and TIMP3 (Cat#: MAB973, R&D Systems, Inc. Minneapolis, MN, USA).

RNA analyses

Endometrial biopsies not used for IHC were thawed in 10 volumes of TRIzol reagent (Invitrogen, Carlsbad, CA, USA) followed immediately by homogenization with a Polytron Tissue Homogenizer (Brinkmann Instruments, Westbury, NY, USA). Total RNA was isolated following the TRIzol protocol (Invitrogen). Following precipitation with ethanol, samples were applied to RNeasy mini kit columns (Qiagen, Valencia, CA, USA). RNase-free DNase digestion was performed on the columns according to the manufacturer's instructions (Qiagen). Total RNA concentrations were quantified by a Nanodrop ND-1000 (Thermo Scientific).

Primers and probes for real-time PCR were designed using Primer Express software (Applied Biosystems, Inc., Carlsbad, CA, USA) based on sequences for each transcript in the NCBI database and validated for use in macaque samples (Keator *et al.*, 2011). See Supplemental Table SI for list of real-time PCR primers and probes. Real-time PCR was performed as previously described (Keator *et al.*, 2011; Almeida-Francia *et al.*, 2012). After reverse transcription of total RNA (1 μg), samples were diluted 1:1 with deionized water. Real-time PCR assays were performed with duplicate samples of 2 μl diluted cDNA, and compared against a standard curve composed of a five-point pool of endometrial cDNA made by a 1:10 serial dilution. A no-template control sample, in which water replaced the cDNA, was used in duplicate for each plate to identify contamination. Each reaction contained 250 nM TaqMan probe specific for gene of interest and for mitochondrial ribosomal protein S10 (see Supplementary Table SI). Each reaction also each contained 900 nM of primer for each gene of interest, 300 nM housekeeping gene sense and antisense primers, and 5 μl of 2× Fast Universal PCR Master Mix (Applied Biosystems, Inc.). Gene transcript was normalized to the expression of S10 and the values were averaged to give a single expression level for each time point during the cycle as previously described (Nolan *et al.*, 2006).

Statistics

For this study, power analysis was performed using a Fisher's Exact test (binomial distribution; statpages.org). We expected 30% of control and 90% of T+WSD females would develop PCO morphology visible by 3D/4D ultrasound in at least one ovary after 3+ years of treatment based on pilot studies (Bishop *et al.*, 2016). Significance for α was set at 0.05, and β of 0.2 (80% power). This analysis revealed a minimum number of nine females are required in each control and treatment group. We chose to treat 10 in each group to avoid failure due to random abnormal cycles.

Individual area under the curve (AUC) values were derived from E2 levels during the early follicular phase, the mid-cycle E2 surge, plus P4 levels during the luteal phase using the Peak Analyzer function of Origin Software (Origin 2016, Origin Lab Corporation, Northampton, MA, USA). The Linear Models function of SAS was used to determine the main effects of androgen (T), diet (WSD), and interaction of T and WSD (androgen by diet) at single time-points (SAS version 9.4, SAS Institute Inc., Cary NC, USA). The effects of T, WSD and interaction (T by WSD) on ovarian morphology (PCOM) was analyzed by Generalized Linear Models function of SAS (chi-squared values were interrogated for level of significance). Longitudinal data were analyzed by Mixed Models function of SAS to evaluate changes induced by T and/or WSD over defined periods of time. When main effects of T, WSD, or interactions were identified as significant ($P < 0.05$), *post-hoc* analyses were performed by least-squared means to identify significant ($P < 0.05$) differences between treatment groups (C, T, WSD and T+WSD; SAS). All values reported are mean ± standard error of the mean (SEM).

Results

Menstrual cycles

Metabolic and adipose alterations induced by chronic T and/or WSD treatment were reported in companion manuscripts (True *et al.*, 2017; Varlamov *et al.*, 2017). Females displayed menarche 3.6 ± 0.6 months after the start of treatment (at 2.6 ± 0.1 years of age; Table I). All females had low E2 and P4 levels in serum at the time of study assignment (Table I). Although females were randomly assigned to groups to ensure a normal distribution of pre-treatment weight between groups, those consuming the normal diet (C and T groups) underwent menarche slightly earlier than those consuming the WSD (WSD and T+WSD; overall effect of diet, $P < 0.04$). However, there were no differences detected in age at menarche between treatment groups (all group differences, i.e. C versus T, etc., $P > 0.3$). As expected, the number of menstrual cycles per year and cycle regularity increased in each group with age after menarche (Table I), but there were no differences detected by androgen or diet treatment on number or length of menstrual cycles, or cycle variation (variation measured by both standard deviation in cycle length and coefficient of variation, data not shown). Weekly analyses of serum P4 levels demonstrated that ~90% of menstrual cycles were presumably ovulatory in Study Year 3 (Table I). Nevertheless, there were no differences in total number or percentage of ovulatory cycles between treatment groups (Table I).

Detailed analyses of a randomly selected menstrual cycle during Study Year 3 determined there were no differences between treatment groups in the length of the follicular phase ($P > 0.5$) or the total E2 (AUC) produced during the follicular phase ($P > 0.3$, data not shown). However, an interaction was detected ($P < 0.02$) between androgen and diet in E2 levels during the early follicular phase (EFP; Fig. 1A): E2 levels were increased by T but decreased by T+WSD (androgen by diet, $P < 0.05$). EFP levels of LH were likewise increased by T alone (Fig. 1B, C versus T, $P < 0.04$), although T+WSD also tended to increase LH compared to C (Fig. 1B, C versus T+WSD, $P = 0.09$; overall effect of androgen, $P < 0.06$). There were no significant effects of androgen or diet on EFP AMH, peak E2, surge E2 (AUC), EFP FSH, or LH:FSH ratio (all $P > 0.3$, data not shown).

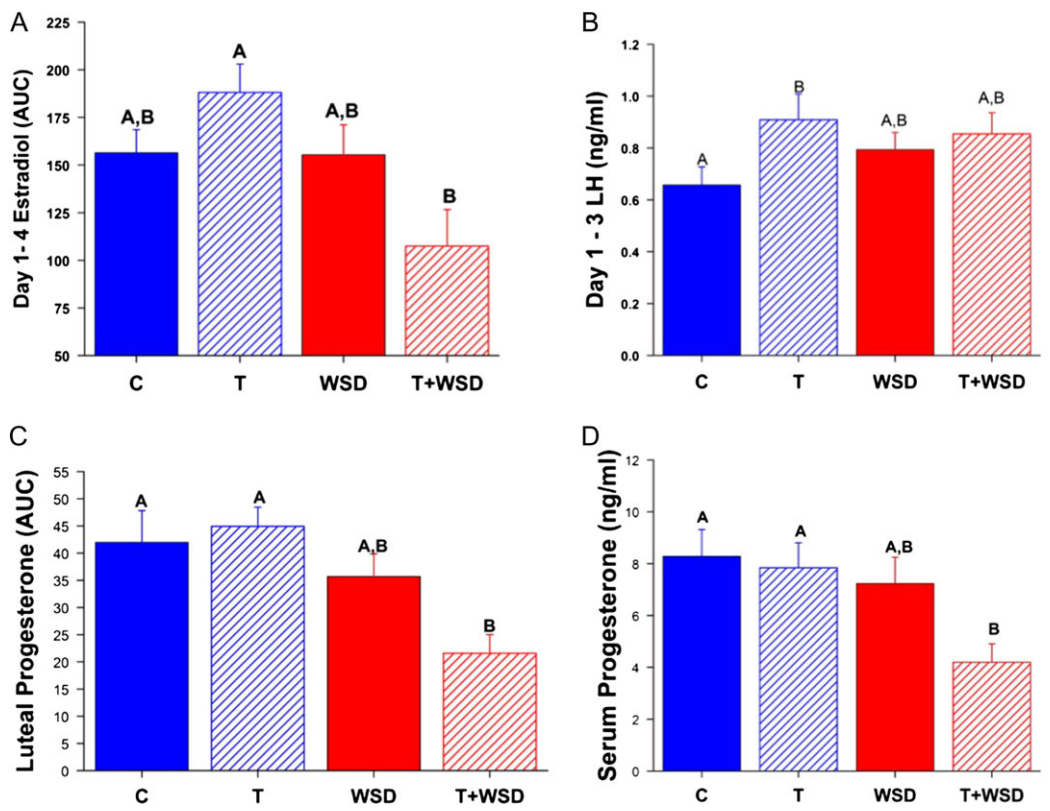

Figure 1 Hormone values from the menstrual cycle analyzed in Study Year 3. Panel (**A**) Estradiol production in the early follicular phase as measured by area under the curve (AUC) on Days 1–4 of the cycle. Panel (**B**) Early follicular phase LH measured on Days 1–3 of the cycle. Panel (**C**) Progesterone production during the luteal phase as measured by AUC from the mid-cycle LH surge to onset of menstruation. Panel (**D**) Peak level of serum progesterone measured during the luteal phase. Significant ($P < 0.05$) differences between treatment groups are denoted by different uppercase letters above columns. C, control; T, testosterone: WSD, western-style diet.

Most females in all treatment groups (9–10/group) displayed elevated P4 levels (>1 ng/ml) during menstrual cycles analyzed in Study Year 3. The length of the luteal phase in these cycles was not affected by androgen or diet ($P > 0.2$). However, females consuming WSD had lower total P4 (AUC) during the luteal phase, and T+WSD group produced the least P4 compared to C and T groups (Fig. 1C, $P < 0.01$; overall effect of diet, $P < 0.001$). Peak P4 levels in the luteal phase showed similar results: females consuming WSD had lower levels of P4 (Fig. 1D, effect of diet, $P < 0.02$), and T+WSD group had the lowest peak P4 levels during the luteal phase compared to C and T groups (Fig. 1D, $P < 0.04$).

Ovarian parameters

3D/4D ultrasound indicated that 30% of C monkeys had PCOM in at least one ovary (Table II). However, treatment with androgen alone (T group) increased incidence to 80%. WSD alone increased the rate of PCOM to 50%, and the T+WSD group had the highest incidence of PCOM at 90% (effect of androgen, $P < 0.01$). The ovaries of WSD and T+WSD groups tended to be larger near menses (Fig. 2A, effect of diet, $P < 0.07$). An interaction was detected between androgen and diet on the number of small antral follicles (SAFs greater-than or equal to 1 mm) present on ovaries at menses (Fig. 2B, $P < 0.05$): T+WSD females had greater numbers of SAFs identified by ultrasound imaging (T versus T+WSD, $P < 0.09$).

Table II Prevalence of polycystic ovarian morphology (PCOM) in the C, T, WSD and T+WSD groups.

Treatment	No PCOM	PCOM*		% PCOM
		One Ovary	Both Ovaries	
C	7	1	2	30[a]
T	2	5	3	80[b]
WSD	5	3	2	50[a,b*]
T+WSD	1	6	3	90[b**]

*PCOM determined by ultrasound imaging: localization of small antral follicles (<2.5 mm) to the outer periphery of the ovary.
[a] versus [b] $P < 0.04$; * versus ** $P = 0.07$.

An increase in BV between the ovary bearing the ovulating follicle and the functional corpus luteum (CL) at mid-luteal phase was only detected in C females (Fig. 3A: C Late F versus Luteal, $P < 0.001$). In all other groups, no increases were significant (Late F versus Luteal,

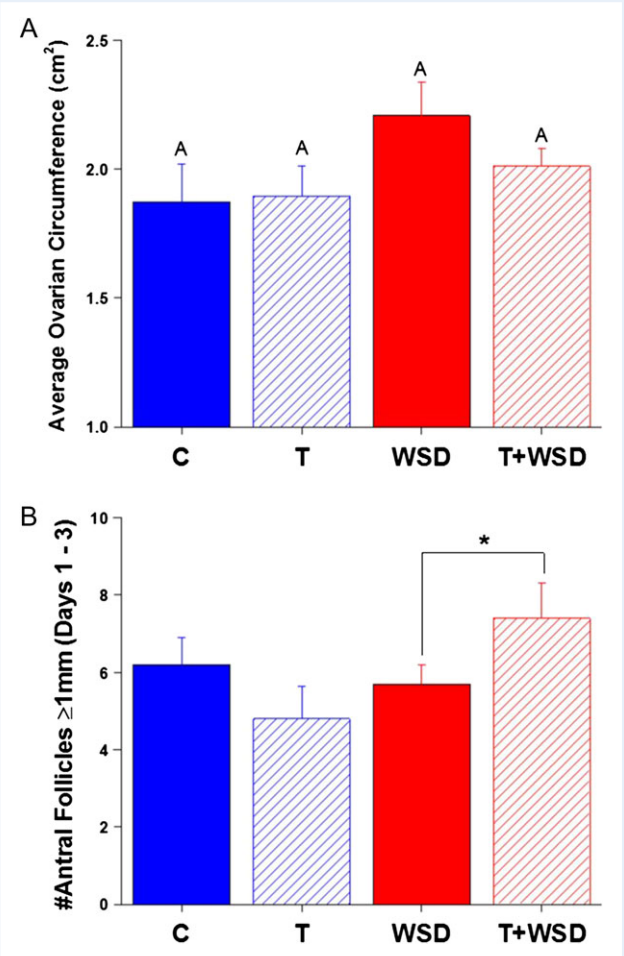

Figure 2 Ovarian morphology during the early follicular phase (Days 1–3) of the cycle. Panel (**A**) average circumference of both ovaries; Panel (**B**) total number of antral follicles ≥1 mm present on ovaries of female monkeys determined by transabdominal 3D/4D US analyses. Significant ($P < 0.05$) differences between treatment groups are denoted by different uppercase letters above columns. Trends toward differences (*$P = 0.09$) between groups are indicated by bracket above relevant comparisons on graphs.

$P > 0.2$). Overall, consumption of the WSD was associated with reduced BV within the CL (Fig. 3A, $P < 0.02$). However, the T alone group also displayed reduced luteal BV (C versus T, $P < 0.02$; androgen by diet interaction, $P < 0.01$). Similarly, only the C group displayed increased ovarian VF at mid-luteal phase (Fig. 3B, $P < 0.02$). However, both WSD and T+WSD treatments tended to reduce luteal VF (effect of diet, $P < 0.13$). Parametric maps of ovarian VF and BV at mid-luteal phase (from ovaries with median values) confirmed incomplete formation of luteal vascular structure in T, WSD and T+WSD groups compared to C ovaries (Fig. 3C).

Uterine parameters

As expected, endometrial volume increased from the late follicular phase to mid-luteal phase in the C group (Fig. 4A). This pattern was less evident in the T and WSD alone groups. However, the pattern was prominent in the T+WSD group, primarily because of low endometrial volume during the late follicular phase of the menstrual cycle (interaction: androgen by diet by phase of the cycle, $P < 0.03$). In the basalis/junctional zone of the uterus T and WSD tended to reduce BV (Fig. 4B; androgen by diet interaction, $P < 0.06$), but this reduction became more pronounced in the endometrium (Fig. 4C; androgen by diet, $P < 0.02$), with BV lowest in the endometrium of the T group (C versus T, $P < 0.05$). Exposure to androgen significantly reduced VF only in the basalis/junctional zone (Fig. 4D; effect of androgen, $P < 0.05$), with no detected effects of androgen or diet on VF in the endometrial tissue (Fig. 4F; all $P > 0.3$).

The endometrial biopsies provided sufficient sample to analyze secretory differentiation induced by P4. Representative examples of ESR1, PGR, TIMP3, MMP26, AR and Ki-67 immunostaining in the endometrial functionalis zone from mid-luteal phase biopsies are shown in Fig. 5. The C and WSD groups displayed typical secretory glands with normal P4-induced attenuation of ESR1 and PGR in the functionalis zone glands. Staining for PGR was retained in the stroma. In these groups, TIMP3 staining was strong in the predecidual cells around the spiral arteries and MMP26 staining was strong in the glands of the upper functionalis zone. In contrast, treatment with T and T+WSD resulted in glands with less secretory sacculation and more intense staining for ESR1 and PGR in the glands, and proportionately less nuclear staining for PGR in the stroma. This outcome was most evident in the T+WSD group. TIMP3 staining was strikingly lighter around the spiral arteries and MMP26 staining was minimal in glands of T and T+WSD animals.

In all groups detectable staining for ESR1 and PGR was retained in cells within the basalis zone (not shown). Expression of AR protein was detectable in the stromal cells of all groups and appeared to be unaffected by treatment (Fig. 5). Cell proliferation, as detected by positive staining for Ki-67 protein, was minimal in the functionalis zone glands of all groups (Fig. 5), with large numbers of proliferating cells in the basalis zone (not shown).

Expression of mRNAs encoding ESR1, PGR, MMP26 and TIMP3 gene products are depicted in Fig. 6. In the C and WSD groups ESR1 and PGR mRNA expression was minimal, whereas MMP26 and TIMP3 transcripts were highly expressed. Treatment with T and T+WSD resulted in an increase in mRNAs encoding ESR1 and PGR ($P < 0.05$). Conversely, T+WSD resulted in a down regulation of MMP26 and TIMP3 mRNAs ($P < 0.05$). Treatment with T alone tended to reduce MMP2 and TIMP3 mRNAs. Expression of AR mRNA was found to not differ by diet and/or T exposure ($P > 0.1$, data not shown).

Discussion

This study was initiated to investigate the chronic effects of hyperandrogenemia, alone and in combination with a western-style (high-fat) diet on the structure-function of the reproductive system in young adult female macaques. The androgen (testosterone, T) dosing was formulated to approximate the 3–4-fold increase in free and total T circulating in hyperandrogenemic peripubertal girls at risk for PCOS (Silfen *et al.*, 2003; McCartney *et al.*, 2007). With an improved immunoassay, as confirmed by LC-MS techniques, it appears that the achieved serum T level of 1.35 ng/ml represents a 5-fold increase over control (C) levels (True *et al.*, 2017). Nevertheless, the T levels of treated animals are much lower than levels observed in male

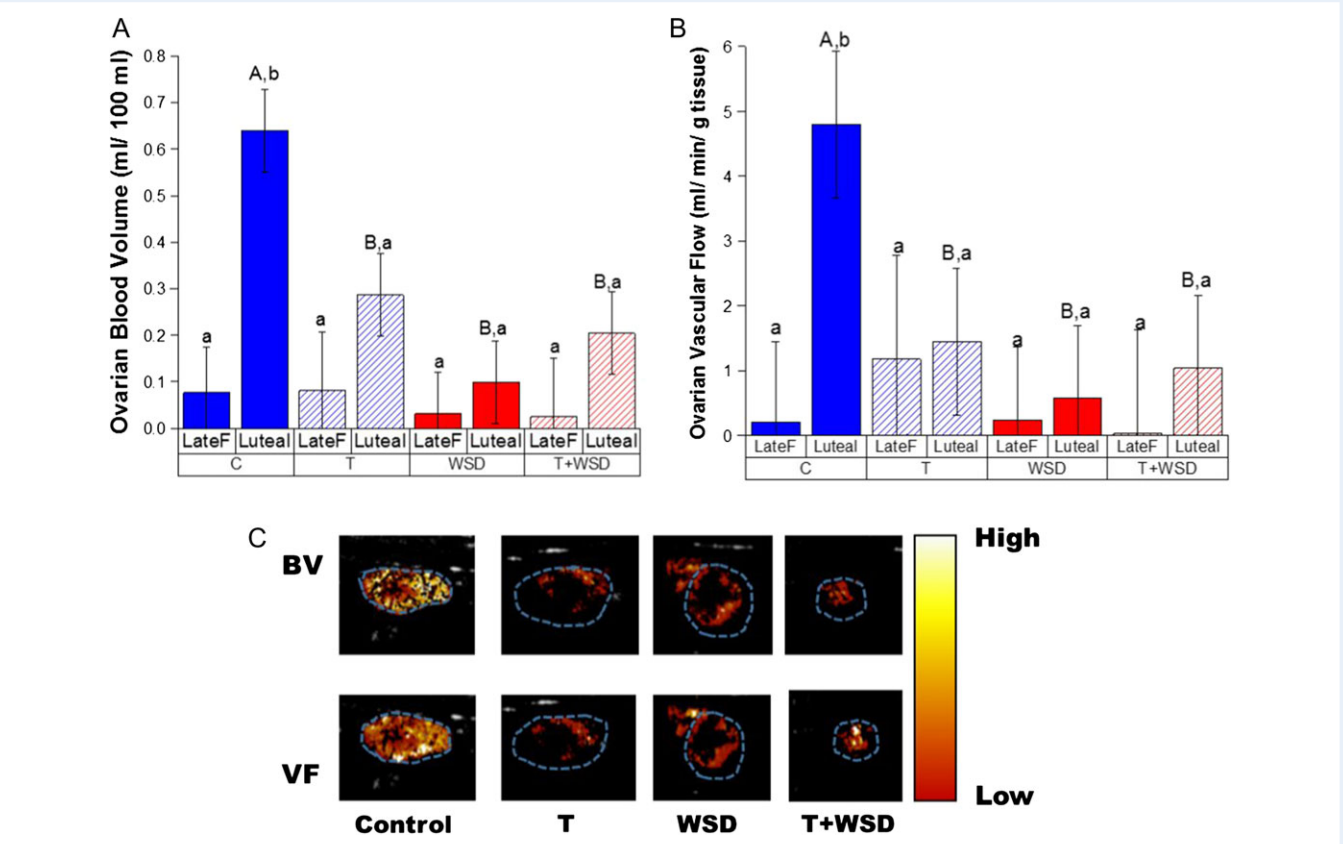

Figure 3 Changes in ovarian vascular function between the late follicular (Late F, prior to mid-cycle LH surge) and mid-luteal (Luteal, Days 6–8 post-LH surge) phases of the menstrual cycle. Panel (**A**) ovarian blood volume (BV) and Panel (**B**) vascular flow (VF) measured by CEUS within the four treatment groups. Panel (**C**) heatmaps of BV and VF are depicted from representative ovaries in each treatment group (median value) at mid-luteal phase. Blue dotted outline depicts ovarian area. Significant ($P < 0.05$) differences between individual treatment groups are denoted by different upper-case letters above columns, and significant ($P < 0.05$) differences within a treatment group by stage of menstrual cycle are denoted by different lower case letters.

macaques (Sitzmann *et al.*, 2014), yet similar to levels some reported in obese PCOS patients (Eagleson *et al.*, 2003). The WSD regimen was designed to mimic a typical American diet and, while containing 2.4-fold more calories as fat than the standard monkey chow, it has many fewer calories from fat (36%) compared to the high-fat diets (up to 60%) often used in rodent studies (Hariri and Thibault, 2010). Our working hypothesis is that the metabolic dysfunction caused by consuming a WSD will exacerbate the effects of hyperandrogenemia, thereby increasing the number or severity of symptoms perhaps similar to those in PCOS. Recent reports by this interdisciplinary group summarized the effects of up to 3 years of treatment on metabolic parameters and adipose tissue (Varlamov *et al.*, 2017). The current manuscript, along with a concluding study (Bishop *et al.*, 2017c) summarize the treatment effects on the structure-function of the reproductive tract, specifically to the ovary and uterus, two recognized targets of androgen action (Cloke and Christian, 2012; Prizant *et al.*, 2014).

Given the experimental design where treatments began just before puberty, a difference in the age at menarche was not expected between groups. Moreover, as noted in adolescent girls (Rosenfield, 2013), the number of menstrual periods increased and the duration of the menstrual cycle decreased over the first 2 years post-menarche. As such, between 4.5 and 5.5 years of age, these young adult females were exhibiting regular cycles (8 or 9 per 9-month interval, excluding the anovulatory summer months (Wilson *et al.*, 1987)), of normal length (approx. 90%, based on elevated progesterone circulating during the luteal phase). Neither T nor WSD treatment alone or in combination altered these parameters of menstrual cyclicity.

However, significant changes to cyclic ovarian structure-function were noted after chronic (3 years) treatment. First, T treatment alone, and to a lesser extent as T+WSD, increased mean LH, but not FSH levels during the early follicular phase. A subtle, but significant, rise in basal LH levels leading to an increased LH:FSH ratio is often observed in PCOS women with hyperandrogenemia (Dumesic *et al.*, 2015; Rosenfield and Ehrmann, 2016). This trend has been attributed to an increase in LH pulse frequency during the early follicular phase, and reduced steroid (E2, P4) feedback inhibition (Rebar *et al.*, 1976). In our pilot study (McGee *et al.*, 2012), T treatment beginning earlier in childhood (1 year of age) increased LH pulse frequency at age five compared to controls, but with addition of a WSD (at age 5.5 and 6.6 years) this increment was lost in association with a marked decline in LH pulse amplitude (McGee *et al.*, 2014). Again, there is some

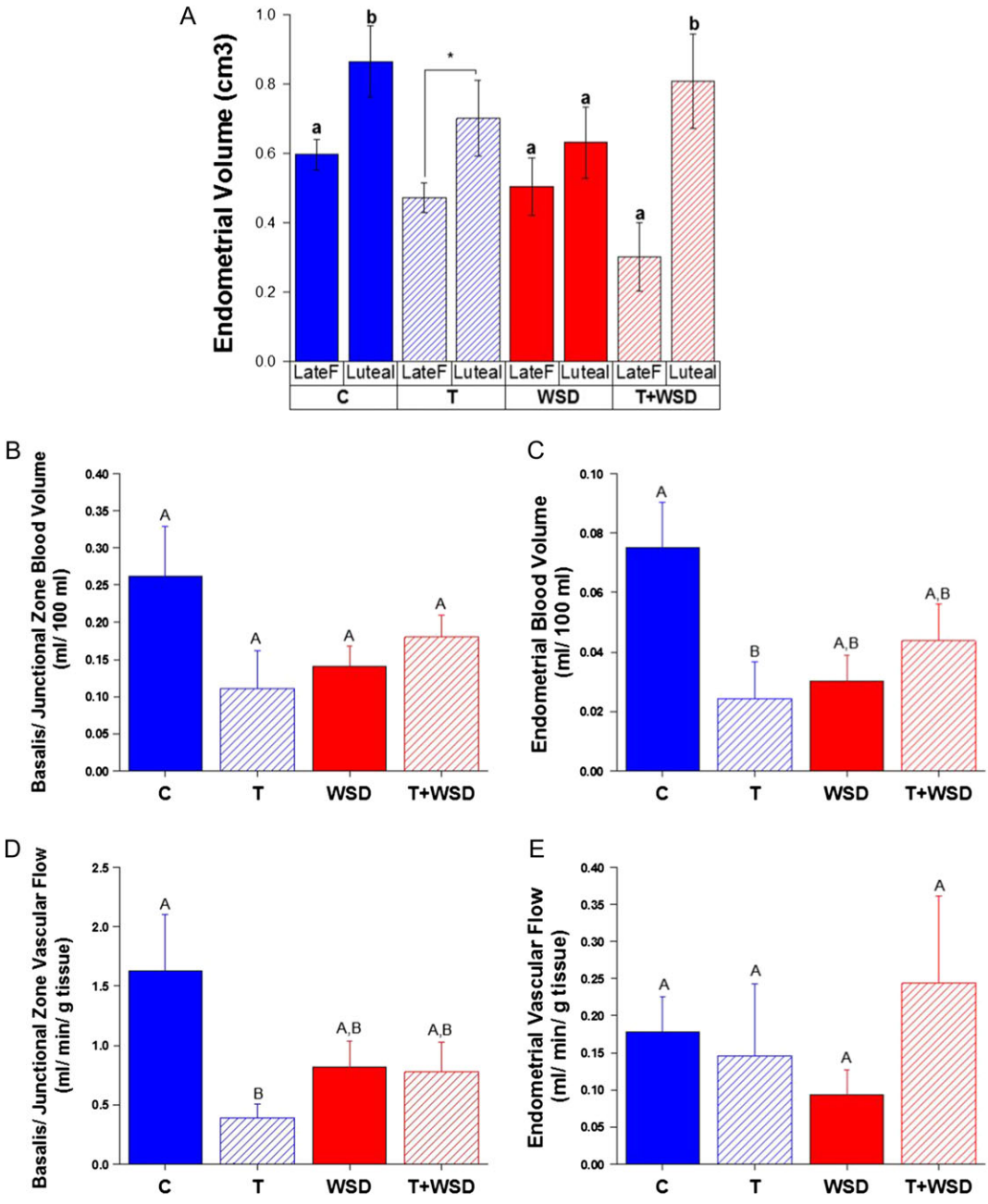

Figure 4 Changes in uterine structure and vascular function induced by hyperandrogenemia and/or WSD (Panel **A**) change in endometrial volume between late follicular (prior to LH surge; Late F)/proliferative and mid-luteal/secretory phase (Luteal, Days 6–8 post-LH surge) of menstrual cycles. Panel (**B**) basalis/junctional zone BV measured by CEUS at mid-luteal phase. Panel (**C**) endometrial BV measured by CEUS at mid-luteal phase. Panel (**D**) basalis/junctional zone VF measured by CEUS at mid-luteal phase. Panel (**E**) endometrial VF measured by CEUS at mid-luteal phase. Significant ($P < 0.05$) differences between individual treatment groups are denoted by different uppercase letters above columns, and significant ($P < 0.05$) differences within a treatment group by stage of menstrual cycle are denoted by different lower case letters. Trends toward differences (*$P = 0.08$) by stage of the cycle within the T group is indicated by a bracket on the graph.

evidence from PCOS patients that obesity can be associated with a decrease in LH pulse amplitude. In the current study, the 40 monkeys were not chronically catheterized, thereby preventing LH pulse studies. However, GnRH and kisspeptin challenge tests were performed to assess pituitary (gonadotrope) and hypothalamic (GnRH neuron) sensitivity to stimulators, and to consider any effects of T or WSD treatment (Supplementary Fig. S2, methods in Supplementary material). Kisspeptin administration during the early follicular phase transiently increased circulating LH levels 4–5-fold, but there were no differences between treatment groups. GnRH administration in the subsequent luteal phase also transiently increased LH levels. Whereas T treatment alone appeared to modestly increase mean LH levels in

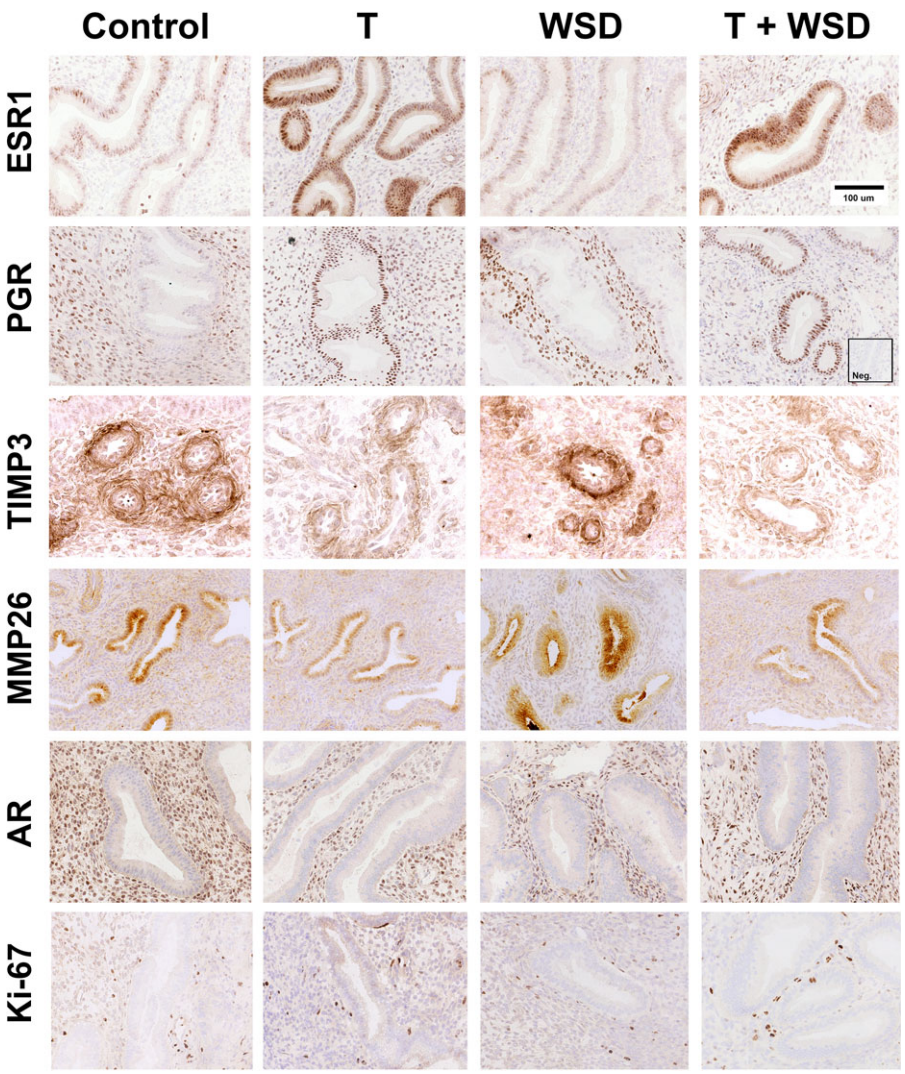

Figure 5 Photomicrographs illustrating immunohistochemical staining for estrogen receptor 1 (ESR1), progesterone receptor (PGR) MMP26, TIMP3, Ki-67 and androgen receptor (AR) in the endometrial functionalis zone of the macaque uterus from representative females in each treatment group (C, T, WSD, T+WSD). Brown staining denotes positive expression of proteins. Sections are counterstained with hematoxylin (blue) staining. ESR1, PGR, Ki-67 and AR staining is nuclear, while MMP26 and TIMP3 show cytoplasmic localization. Inset shows a negative control with an irrelevant antibody (Anti-Br(d)U). TIMP3 staining was localized to the predecidual cells around the spiral arteries.

response to GnRH (2-fold compared to controls or other treatments), due to wide variation in response by the T group this difference was not statistically significant ($P > 0.05$). The cause(s) of altered LH levels in the T group during the early follicular phase remain speculative.

The modest elevation in circulating LH in the T alone group was associated with a similar rise in serum E2 levels in the early follicular phase. In contrast, the combined T+WSD group displayed markedly lower E2 levels in the early follicular phase, followed by reduced P4 levels during the luteal phase. These results are comparable to those observed in the T+WSD group in our pilot study (McGee *et al.*, 2014). Low E2 levels during the follicular phase are associated with luteal phase defects in women (Schliep *et al.*, 2014), and are consistent with the concept that a follicular defect may portend luteal dysfunction. Women with PCOS can have low P4 levels during the luteal phase in spontaneous or controlled stimulation cycles compared to non-PCOS controls (Meenakumari *et al.*, 2004). Similarly, female macaques given exogenous androgen during pregnancy yielded offspring with an increased incidence of luteal phase defects during menstrual cycles (Goy and Robinson, 1982). It is important to note that, despite the lower P4 levels in the T+WSD group, they were not sufficiently depressed to cause premature menstruation, i.e. short luteal phases more associated with fertility problems in women (Schliep *et al.*, 2014).

The cause of diminished luteal function is unclear, but not likely due to reduced trophic hormone support, since LH levels during the luteal phase were similar in all treatment groups. In contrast, this study provides novel evidence that T and WSD, both alone and in combination, markedly blunt the rise in ovarian vascular perfusion associated with

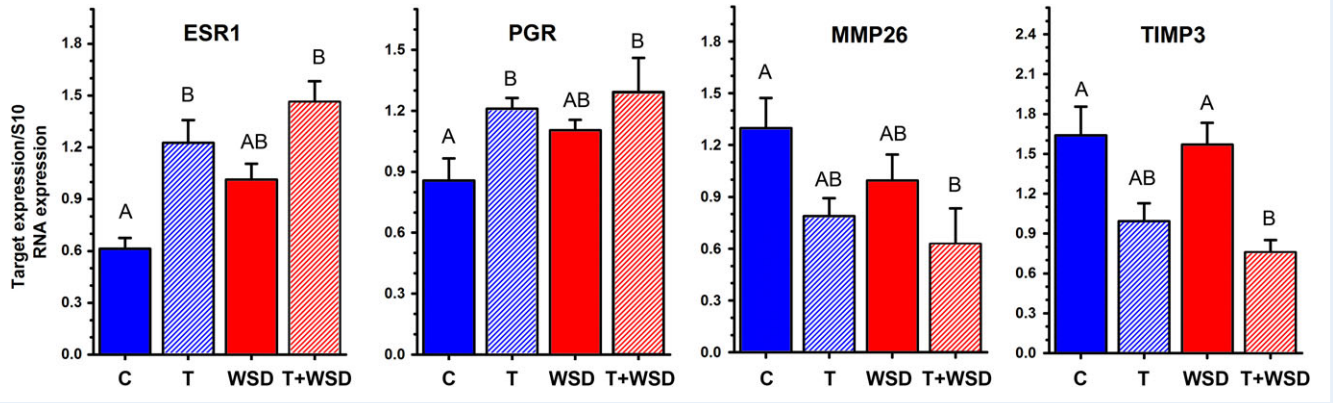

Figure 6 Expression of ESR1, PGR, MMP26 and TIMP3 mRNAs as detected by qRT-PCR in endometrial biopsies collected from macaques in the mid-luteal phase of the cycle. Significant ($P < 0.05$) differences between individual treatment groups are denoted by different uppercase letters above columns.

neovascularization of the developing corpus luteum during the luteal phase of the cycle (Bishop *et al.*, 2014; Woad and Robinson, 2016). Both blood volume (an indicator of the vascular tree) and blood flow (an indication of vascular function) are markedly reduced, indeed similar to late follicular phase with its preovulatory follicle during T and/or WSD treatment. Such a decline in vascular function could influence the endocrine secretory activity of the corpus luteum, e.g. reducing serum P4 levels as observed in the T+WSD group. However, P4 levels were not reduced in the T and WSD alone groups despite marked reductions in ovarian blood volume and flow. Further studies are needed to evaluate the effects and significance of T and WSD (metabolic) actions on the vasculature of the primate reproductive tract.

More direct evidence of a follicular defect(s) with T treatment was the greater incidence (80–90% of monkeys) of a PCOM in the T alone and T+WSD groups. We previously observed this feature in our pilot study (Bishop *et al.*, 2016), especially with addition of WSD to chronic T treatment. Subsequent removal of ovaries in the early follicular phase and further histologic analyses confirmed the presence of increased numbers of small antral follicles, many of which were atretic compared to untreated controls in our colony. While later protocols may yield ovaries from the current treatment cohorts, to date we have obtained histology from ovaries of only one T+WSD-treated animal when she was euthanized after 3 years of because of progressing oral cancer. These ovaries also displayed an abundance of small-to-medium antral follicles around the periphery of the ovary (Supplementary Fig. S3). Notably, as in our pilot study (Bishop *et al.*, 2016), 30% of the C females also exhibited a PCOM-like ovarian phenotype. This is similar to clinical data demonstrating that 26% of young, asymptomatic women display a PCOM phenotype (Polson *et al.*, 1988; Bridges *et al.*, 1993), although it was proposed that these women have mild or early onset PCOS (Rosenfield and Ehrmann, 2016). The WSD may also have some effects on the follicular pool since ovarian size was greatest in the high-fat diet groups and WSD alone resulted in intermediate percentage (50%) of animals with PCOM. Further studies are warranted to detail the follicular dynamics in T and WSD-treated monkeys.

Progesterone (P4) secreted in the luteal phase of the cycle prepares the estrogen-primed endometrium for embryo implantation. During this interval, P4 gradually suppresses epithelial cell proliferation in the functionalis zone glands, induces glandular hypertrophy and reduces ESR1 and PGR staining in the functionalis zone (Slayden, 2014). At the same time, P4 stimulates MMP26 expression in the functionalis zone glands (Almeida-Francia *et al.*, 2012), and TIMP3 expression in the predecidual cells surrounding the spiral arteries (Brenner *et al.*, 2006). This is the state observed with the C and WSD-treated animals in this study. However, treatment of macaques with T and T+WSD in this study resulted in a partial impairment of this process with ESR1 being retained in the glandular epithelium. Elevated ESR1 in the mid-secretory phase has been reported and associated with impaired uterine recepitivity in women (Lessey *et al.*, 2006). Mild dysregulation of ESR1 expression (both protein and mRNA transcript) combined with the attenuation of MMP26 and TIMP3 in the secretory phase of T and T+WSD-treated females can be interpreted as a mild P4 resistance similar to that seen in early stages of endometriosis (Burney *et al.*, 2007). However, the effect of T and T+WSD appears to be only superficial as both secretory differentiation and P4-induced suppression of cell proliferation appeared normal for the mid-secretory phase of the cycle. Increased expression of ESR1 and PGR is also reported in the endometrium of PCOS women, but these are thought to be the result of exposure to repeated anovulatory menstrual cycles (Piltonen, 2016). These data demonstrate that chronic hyperandrogenemia alters expression of these receptors in nonhuman primates during ovulatory cycles as well.

Collectively, the results reported in the current and two previous papers (True *et al.*, 2017; Varlamov *et al.*, 2017) identified significant effects of chronic hyperandrogenemia and WSD on the reproductive system, metabolic function and adipose tissue in young, adult female monkeys. Whereas some changes were noted following T alone (e.g. PCOM, decreased physical activity, reduced lipolysis) or WSD alone (e.g. decreased ovarian blood flow, reduced length and numbers of adipose tissue vessels and junctions), the combination of T+WSD increased the number of changes or magnified the effects (e.g. increased BMI, fat mass and insulin resistance, increased fatty acid uptake by fat; luteal insufficiency). Nevertheless, these young, adult females appear relatively healthy (e.g. euglycemic, regular menstrual cycles). Also, some PCOS symptoms, including loss of menstrual

cyclicity and elevated serum AMH levels were not observed. The latter may be causally related to the continued selection of a preovulatory follicle, which is associated with declining AMH production by antral follicles (Xu *et al.*, 2016b), and may be required for selection of the single, dominant follicle destined to ovulate (Xu *et al.*, 2016a). Ongoing studies will determine if T and/or WSD effects increase in number or severity with longer treatment into adulthood due to continued hyperandrogenemia and/or higher rate of obesity. Not all T+WSD females are extremely overweight/obese, and most WSD-treated females are within normal weight range at this young age, but continued exposure to WSD is expected to result in higher rates of adiposity as females age and are less active. Also, it is hypothesized that changes in ovarian (luteal phase dysfunction; oocyte quality as suggested by our concluding study of the peri-ovulatory follicle (Bishop *et al.*, 2017c)) and uterine endometrium (suppressed markers of progesterone action, impaired decidualization) could impair fertility, or pregnancy progression. Frias *et al.* (2011) report that WSD alone in adult, female macaques causes placental dysfunction and stillbirths; the combination of T+WSD may exacerbate such problems (Bishop *et al.*, 2017b).

Supplementary data

Supplementary data are available at *Human Reproduction* online.

Acknowledgements

The authors are grateful for the critical support of the ONPRC Surgical Services Unit staff under direction of Theodore Hobbs, DVM, for assistance with execution of all animal studies. Equipment and technical support for contrast-enhanced ultrasound studies was graciously provided by Dr. Jonathan Lindner, MD, Chief, Division of Cardiometabolic Health, ONPRC and Todd Belcik, MS, Senior Research Associate Knight Cardiovascular Institute, OHSU. The efforts of ONPRC Endocrine Technology Support Core Lab under direction of Dr. David Erickson are also appreciated.

Authors' roles

CVB contributed to experimental design, oversaw execution of experimental protocols/data acquisition and performed nonhuman primate ultrasonography, data analyses and manuscript preparation. ECM coordinated experimental protocols and data acquisition and provided data analyses. DLT coordinated experimental protocols, data acquisition and data analyses. TER assisted with experimental protocols, contributed to data preparation and provided data analyses. KRB assisted with experimental protocols, data acquisition and provided data analyses. CAT contributed to experimental design, data acquisition and performed data analyses. ODS contributed to experimental design, oversaw execution of experimental protocols/data acquisition, provided data analyses and manuscript preparation. RLS contributed to experimental design, funding of the study, data analysis and manuscript preparation. All authors had final approval of manuscript before publication.

Funding

Research reported in this publication was supported by the Eunice Kennedy Shriver National Institute of Child Health & Human Development (NICHD) of the National Institutes of Health (NIH) under Award Number P50HD071836 (to RLS). The content is solely the responsibility of the authors and does not necessarily represent the official views of the NIH. Additional funding was provided by Office of the Director, NIH under Award Number P51OD011092 (Support for National Primate Research Center).

Conflict of interest

None declared.

References

Almeida-Francia CC, Keator CS, Mah K, Holden L, Hergert C, Slayden OD. Localization and hormonal regulation of endometrial matrix metalloproteinase-26 in the rhesus macaque. *Hum Reprod* 2012;**27**:1723–1734.

Bishop CV, Lee DM, Slayden OD, Li X. Intravenous neutralization of vascular endothelial growth factor reduces vascular function/permeability of the ovary and prevents development of OHSS-like symptoms in rhesus monkeys. *J Ovarian Res* 2017a;**10**:41.

Bishop CV, Mishler EC, Takahashi DL, True CA, Slayden OD, Stouffer RL. Chronically Elevated Androgen With or Without A Western-Style Diet Reduces the Pregnancy Rate and Early Placental Vascularization In Young Adult Rhesus Monkeys. 73rd Annual Meeting American Society for Reproductive Medicine. *American Society for Reproduction Medicine's Annual Meeting*. 2017b, San Antonio, TX, USA, pp. #O-174.

Bishop CV, Molskness TA, Xu F, Belcik JT, Lindner JR, Slayden OD, Stouffer RL. Quantification of dynamic changes to blood volume and vascular flow in the primate corpus luteum during the menstrual cycle. *J Med Primatol* 2014;**43**:445–454.

Bishop CV, Reiter TE, Hanna CB, Daughtry B, Chavez S, Hennebold JD, Stouffer RL. Elevated Androgen and/or Consumption of a Western-Style Diet Has Detrimental Effects on the Rhesus Monkey Ovulatory Follicles and Oocytes. *American Society for Reproduction Medicine's Annual Meeting*. 2017c, San Antonio TX, USA, pp. #O-173.

Bishop CV, Sparman ML, Stanley JE, Bahar A, Zelinski MB, Stouffer RL. Evaluation of antral follicle growth in the macaque ovary during the menstrual cycle and controlled ovarian stimulation by high-resolution ultrasonography. *Am J Primatol* 2009;**71**:384–392.

Bishop CV, Xu F, Xu J, Ting AY, Galbreath E, McGee WK, Zelinski MB, Hennebold JD, Cameron JL, Stouffer RL. Western-style diet, with and without chronic androgen treatment, alters the number, structure, and function of small antral follicles in ovaries of young adult monkeys. *Fertil Steril* 2016;**105**:1023–1034.

Brenner R, Mah K, Tsong Y, Citruk-Ware R, Slayden O. Zonal differences in hormonal responsiveness during decidualization in the primate endometrium. *The Endocrine Society's 88th Annual Meeting*. 2006, pp. 24–27.

Brenner RM, Slayden OD. Steroid receptors in blood vessels of the rhesus macaque endometrium. *Arch Histol Cytol* 2004;**67**:441–446.

Brenner RM, Slayden OD, Rodgers WH, Critchley HOD, Carroll R, Nie XJ, Mah K. Immunocytochemical ssessment of mitotic activity with an antibody to phosphorylated histone H3 in the macaque and human endometrium. *Hum Reprod* 2003;**18**:1185–1193.

Bridges NA, Cooke A, Healy MJ, Hindmarsh PC, Brook CG. Standards for ovarian volume in childhood and puberty. *Fertil Steril* 1993;**60**:456–460.

Brozinick JT, Hawkins E, Hoang Bui H, Kuo MS, Tan B, Kievit P, Grove K. Plasma sphingolipids are biomarkers of metabolic syndrome in non-human primates maintained on a Western-style diet. *Int J Obes (Lond)* 2013;**37**:1064–1070.

Burney RO, Talbi S, Hamilton AE, Vo KC, Nyegaard M, Nezhat CR, Lessey BA, Giudice LC. Gene expression analysis of endometrium reveals progesterone resistance and candidate susceptibility genes in women with endometriosis. *Endocrinology* 2007;**148**:3814–3826.

Cloke B, Christian M. The role of androgens and the androgen receptor in cycling endometrium. *Mol Cell Endocrinol* 2012;**358**:166–175.

Dumesic DA, Oberfield SE, Stener-Victorin E, Marshall JC, Laven JS, Legro RS. Scientific statement on the diagnostic criteria, epidemiology, pathophysiology, and molecular genetics of polycystic ovary syndrome. *Endocr Rev* 2015;**36**:487–525.

Eagleson CA, Bellows AB, Hu K, Gingrich MB, Marshall JC. Obese patients with polycystic ovary syndrome: evidence that metformin does not restore sensitivity of the gonadotropin-releasing hormone pulse generator to inhibition by ovarian steroids. *J Clin Endocrinol Metab* 2003;**88**: 5158–5162.

Frias AE, Morgan TK, Evans AE, Rasanen J, Oh KY, Thornburg KL, Grove KL. Maternal high-fat diet disturbs uteroplacental hemodynamics and increases the frequency of stillbirth in a nonhuman primate model of excess nutrition. *Endocrinology* 2011;**152**:2456–2464.

Goy R, Robinson J. Prenatal exposure of rhesus monkeys to patent androgens: morphological, behavioral, and physiological consequences. *Banbury Rep* 1982;**11**:355–378.

Hariri N, Thibault L. High-fat diet-induced obesity in animal models. *Nutr Res Rev* 2010;**23**:270–299.

Hoeger K, Davidson K, Kochman L, Cherry T, Kopin L, Guzick DS. The impact of metformin, oral contraceptives, and lifestyle modification on polycystic ovary syndrome in obese adolescent women in two randomized, placebo-controlled clinical trials. *J Clin Endocrinol Metab* 2008;**93**: 4299–4306.

Keator CS, Mah K, Ohm L, Slayden OD. Estrogen and progesterone regulate expression of the endothelins in the rhesus macaque endometrium. *Hum Reprod* 2011;**26**:1715–1728.

Lessey BA, Palomino WA, Apparao KB, Young SL, Lininger RA. Estrogen receptor-alpha (ER-alpha) and defects in uterine receptivity in women. *Reprod Biol Endocrinol* 2006;**4**:S9.

McCartney CR, Blank SK, Prendergast KA, Chhabra S, Eagleson CA, Helm KD, Yoo R, Chang RJ, Foster CM, Caprio S *et al*. Obesity and sex steroid changes across puberty: evidence for marked hyperandrogenemia in pre- and early pubertal obese girls. *J Clin Endocrinol Metab* 2007;**92**: 430–436.

McGee WK, Bishop CV, Bahar A, Pohl CR, Chang RJ, Marshall JC, Pau FK, Stouffer RL, Cameron JL. Elevated androgens during puberty in female rhesus monkeys lead to increased neuronal drive to the reproductive axis: a possible component of polycystic ovary syndrome. *Hum Reprod* 2012;**27**:531–540.

McGee WK, Bishop CV, Pohl CR, Chang RJ, Marshall JC, Pau FK, Stouffer RL, Cameron JL. Effects of hyperandrogenemia and increased adiposity on reproductive and metabolic parameters in young adult female monkeys. *Am J Physiol Endocrinol Metab* 2014;**306**:E1292–E1304.

Meenakumari KJ, Agarwal S, Krishna A, Pandey LK. Effects of metformin treatment on luteal phase progesterone concentration in polycystic ovary syndrome. *Br J Med Biol Res* 2004;**37**:1637–1644.

Nolan T, Hands RE, Bustin SA. Quantification of mRNA using real-time RT-PCR. *Nat Protoc* 2006;**1**:1559–1582.

Palomba S, Daolio J, La Sala GB. Oocyte Competence in Women with polycystic ovary syndrome. *Trends Endocrinol Metab* 2017;**28**:186–198.

Piltonen TT. Polycystic ovary syndrome: endometrial markers. *Best Pract Res Clin Obstet Gynaecol* 2016;**37**:66–79.

Polson DW, Adams J, Wadsworth J, Franks S. Polycystic ovaries—a common finding in normal women. *Lancet (London, England)* 1988;**1**: 870–872.

Prizant H, Gleicher N, Sen A. Androgen actions in the ovary: balance is key. *J Endocrinol* 2014;**222**:R141–R151.

Rebar R, Judd HL, Yen SS, Rakoff J, Vandenberg G, Naftolin F. Characterization of the inappropriate gonadotropin secretion in polycystic ovary syndrome. *J Clin Invest* 1976;**57**:1320–1329.

Rosenfield RL. Clinical review: adolescent anovulation: maturational mechanisms and implications. *J Clin Endocrinol Metab* 2013;**98**: 3572–3583.

Rosenfield RL, Ehrmann DA. The pathogenesis of polycystic ovary syndrome (PCOS): the hypothesis of PCOS as functional ovarian hyperandrogenism revisited. *Endocr Rev* 2016;**37**:467–520.

Schliep KC, Mumford SL, Hammoud AO, Stanford JB, Kissell KA, Sjaarda LA, Perkins NJ, Ahrens KA, Wactawski-Wende J, Mendola P *et al*. Luteal phase deficiency in regularly menstruating women: prevalence and overlap in identification based on clinical and biochemical diagnostic criteria. *J Clin Endocrinol Metab* 2014;**99**:E1007–E1014.

Schulte MM, Tsai JH, Moley KH. Obesity and PCOS: the effect of metabolic derangements on endometrial receptivity at the time of implantation. *Reprod Sci* 2015;**22**:6–14.

Silfen ME, Denburg MR, Manibo AM, Lobo RA, Jaffe R, Ferin M, Levine LS, Oberfield SE. Early endocrine, metabolic, and sonographic characteristics of polycystic ovary syndrome (PCOS): comparison between nonobese and obese adolescents. *J Clin Endocrinol Metab* 2003;**88**:4682–4688.

Sitzmann BD, Brown DI, Garyfallou VT, Kohama SG, Mattison JA, Ingram DK, Roth GS, Ottinger MA, Urbanski HF. Impact of moderate calorie restriction on testicular morphology and endocrine function in adult rhesus macaques (Macaca mulatta). *Age Dordr Neth* 2014;**36**:183–197.

Slayden OD. Cyclic remodeling of the nonhuman primate endometrium: a model for understanding endometrial receptivity. *Semin Reprod Med* 2014;**32**:385–391.

Slayden OD, Hettrich K, Carroll RS, Otto LN, Clark AL, Brenner RM. Estrogen enhances cystatin C expression in the macaque vagina. *J Clin Endocrinol Metabol* 2004;**89**:889–891.

Slayden OD, Koji T, Brenner RM. Microwave stabilization enhances immunocytochemical detection of estrogen receptor in frozen sectionf of macaque oviduct. *Endocrinology* 1995;**136**:4012–4021.

True CA, Takahashi DL, Burns SE, Mishler EC, Bond KR, Wilcox MC, Calhoun AR, Bader LA, Dean TA, Ryan ND *et al*. Chronic combined hyperandrogenemia and western-style diet in young female rhesus macaques causes greater metabolic impairments compared to either treatment alone. *Hum Reprod* 2017;**32**:1880–1891.

Varlamov O, Bishop CV, Handu M, Takahashi D, Srinivasan S, White A, Roberts CT Jr. Combined androgen excess and Western-style diet accelerates adipose tissue dysfunction in young adult, female nonhuman primates. *Hum Reprod* 2017;**32**:1892–1902.

Wilson ME, Pope NS, Gordon TP. Seasonal modulation of luteinizing-hormone secretion in female rhesus monkeys. *Biol Reprod* 1987;**36**: 975–984.

Woad KJ, Robinson RS. Luteal angiogenesis and its control. *Theriogenology* 2016;**86**:221–228.

Xu J, Bishop CV, Lawson MS, Park BS, Xu F. Anti-Mullerian hormone promotes pre-antral follicle growth, but inhibits antral follicle maturation and dominant follicle selection in primates. *Hum Reprod* 2016a;**31**: 1522–1530.

Xu J, Xu F, Letaw JH, Park BS, Searles RP, Ferguson BM. Anti-Mullerian hormone is produced heterogeneously in primate preantral follicles and is a potential biomarker for follicle growth and oocyte maturation in vitro. *J Assist Reprod Genet* 2016b;**33**:1665–1675.

Young KA, Chaffin CL, Molskness TA, Stouffer RL. Controlled ovulation of the dominant follicle: a critical role for LH in the late follicular phase of the menstrual cycle. *Hum Reprod* 2003;**18**:2257–2263.